

Supplement of

Combined organic and inorganic source apportionment on yearlong ToF – ACSM dataset at a suburban station in Athens

Olga Zografou, et al.

Correspondence to: Olga Zografou (o.zografou@ipta.demokritos.gr) and Konstantinos Eleftheriadis (elefther@ipta.demokritos.gr)

S1. AE33 black carbon apportionment

The AE33 provides the light absorption coefficients and the respective eBC concentrations (using an appropriate mass absorption cross section number, MAC) at seven wavelengths (370, 470, 520, 590, 660, 880 and 950 nm). In this study, the eBC concentrations are reported at $\lambda=880$ nm (Petzold et al., 2013), considering a MAC number to convert absorption coefficient to eBC concentration equal to $4.6 \text{ m}^2\text{g}^{-1}$ (Kalogridis et al., 2018). Additionally, the AE33 provides the contribution of wood burning and fossil fuel to the total eBC mass concentrations through the application of the Aethalometer model as described by Sandradewi et al. (2008):

$$\frac{b_{abs}(\lambda_{UV})_{ff}}{b_{abs}(\lambda_{IR})_{ff}} = \left(\frac{\lambda_{UV}}{\lambda_{IR}}\right)^{-a_{ff}}, \quad (3)$$

$$\frac{b_{abs}(\lambda_{UV})_{wb}}{b_{abs}(\lambda_{IR})_{wb}} = \left(\frac{\lambda_{UV}}{\lambda_{IR}}\right)^{-a_{wb}}, \quad (4)$$

$$b_{abs}(\lambda_{UV})_{wb} = \left(\frac{1}{1 - \left(\frac{\lambda_{UV}}{\lambda_{IR}}\right)^{-a_{ff}} \left(\frac{\lambda_{UV}}{\lambda_{IR}}\right)^{a_{wb}}}\right) \left(b_{abs}(\lambda_{UV}) - \left(\left(\frac{\lambda_{UV}}{\lambda_{IR}}\right)^{-a_{ff}} b_{abs}(\lambda_{IR})\right)\right), \quad (5)$$

where a_{ff} and a_{wb} are the absorption Ångström exponents for pure fossil fuel combustion and pure wood burning aerosol, respectively; $babs(\lambda_{UV})$ and $babs(\lambda_{IR})$ are the absorption coefficients measured at the UV (470 nm) and IR (950 nm) wavelengths, respectively, with the blue (470 nm) channel found to perform better than the traditionally formulated UV channel (370 nm) in the aethalometer model $babs(\lambda_{UV})_{wb}$ & $babs(\lambda_{IR})_{wb}$ and $babs(\lambda_{UV})_{ff}$ & $babs(\lambda_{IR})_{ff}$ are the corresponding absorption coefficients at these two wavelengths that are related to wood burning (wb) and fossil fuel combustion (ff). According to the earlier sensitivity study for our area a_{ff} and a_{wb} values was found equal to 0.9 and 2 respectively (Diapouli et al., 2017; Kalogridis et al., 2018).

Table S1. List of criteria applied for selecting environmentally reasonable runs.

Factor	Criterion	Threshold
HOA	HOA-eBCff correlation	p<=0.05
COA	Hourly contribution: $\frac{12}{9+10}$	>1
BBOA	SFBOA-eBCwb correlation	p<=0.05
SFBOA	SFBOA-expl.var m60	p<=0.05
LO-OOA	Monitor m/z 43, 44	>0
MO-OOA	Monitor m/z 43, 44	>0

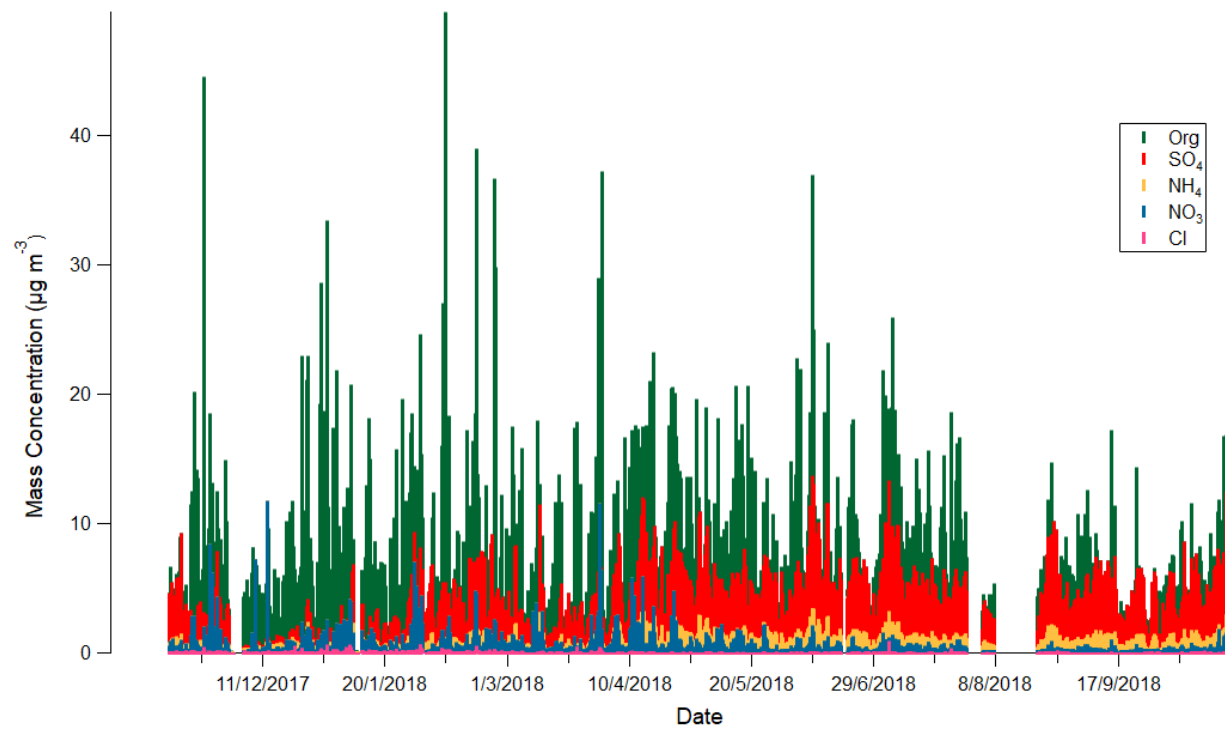
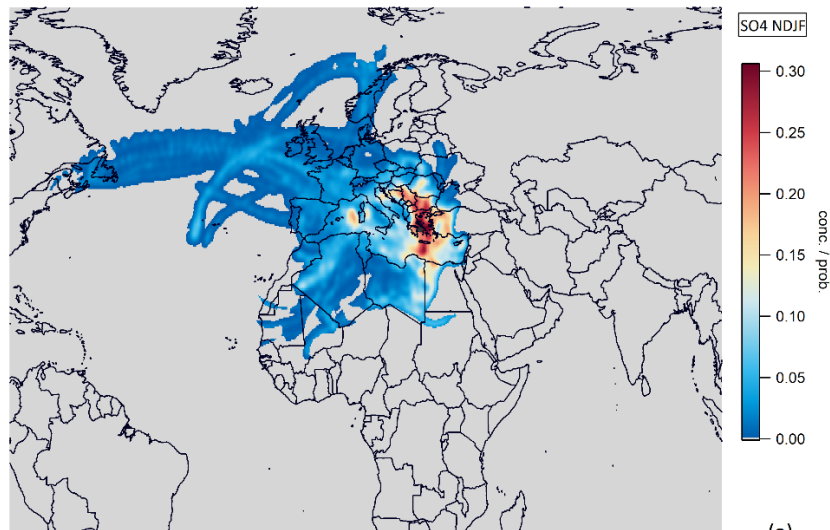


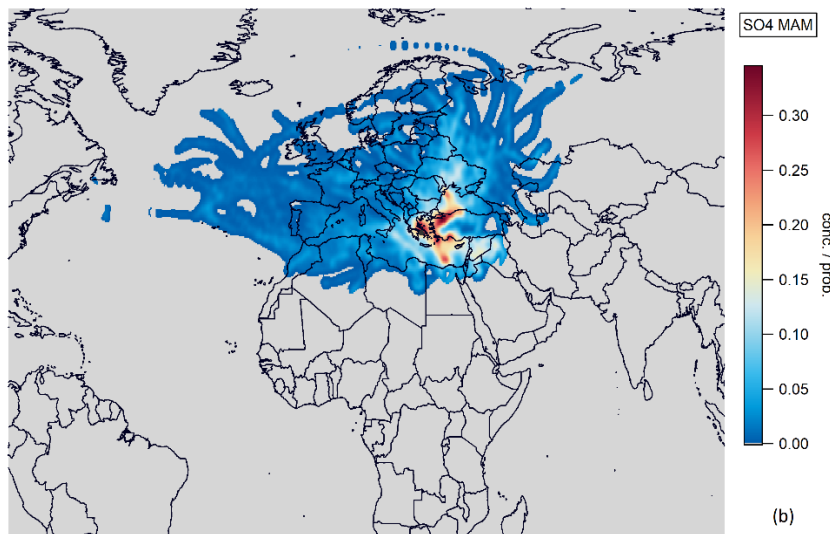
Figure S1. Time Series of the NRS (Organics, sulphate, ammonium, nitrate and chloride) from ToF-ACSM for November 2017 to October 2018.

Table S2. NRS mass concentration in μgm^{-3} for each period reported: (November 2017–February 2018 (NDJF), March–May (MAM), June–August (JJA) and September–October (SO).

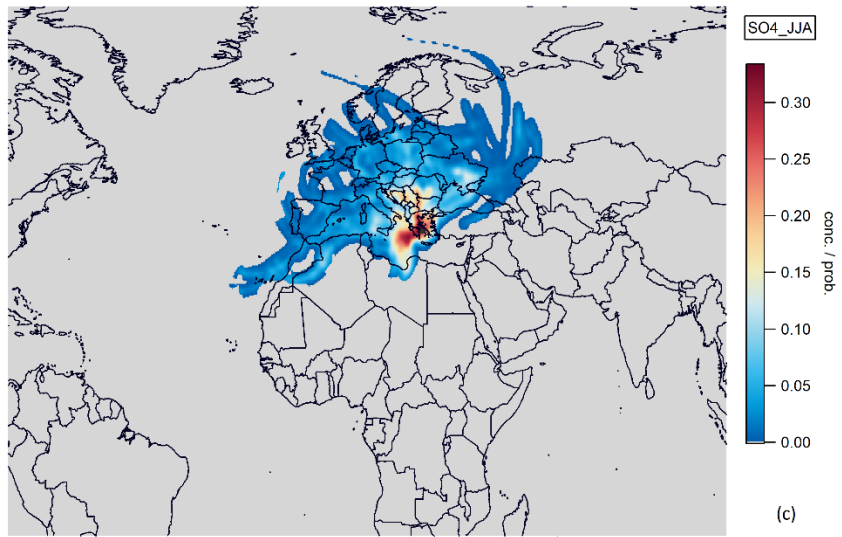
$\mu\text{g m}^{-3}$	Yearly	NDJF	MAM	JJA	SO
Org	4.6	4.11	5.1	5.1	4.7
SO₄²⁻	3.03	2.04	3.45	3.57	3.97
NO₃⁻	0.38	0.47	0.47	0.26	0.28
NH₄⁺	0.82	0.61	0.99	0.87	0.94
Cl⁻	0.02	0.05	0.02	0.02	0.02
eBC	0.82	0.8	0.88	0.76	0.91
PM1	9.67	8.08	10.91	10.58	10.82



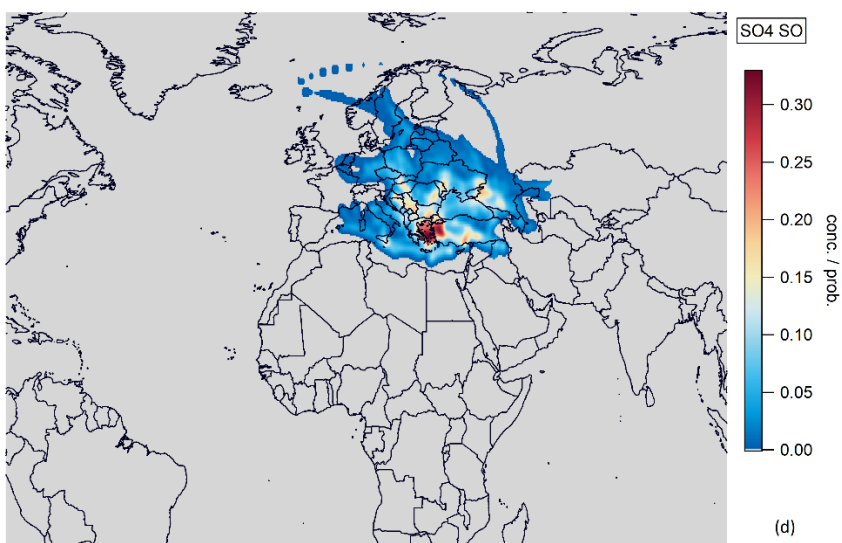
(a)



(b)



(c)



(d)

Figure S2. Back-trajectories for each season for sulfate: NDJF (a), MAM (b), JJA (c) and SO (d)

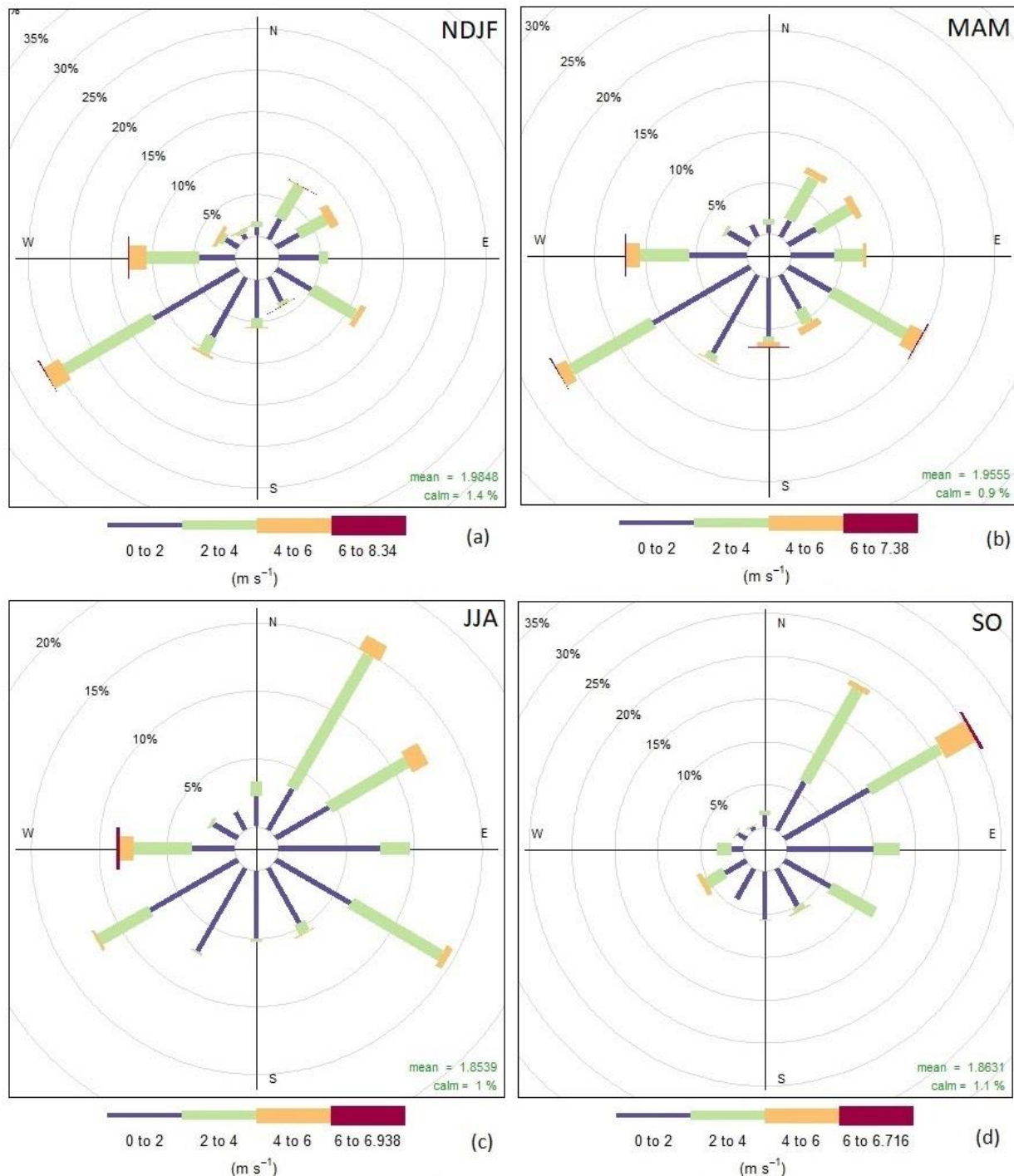


Figure S3. Wind rose plots for each season studied: NDJF (a), MAM (b), JJA (c) and SO (d).

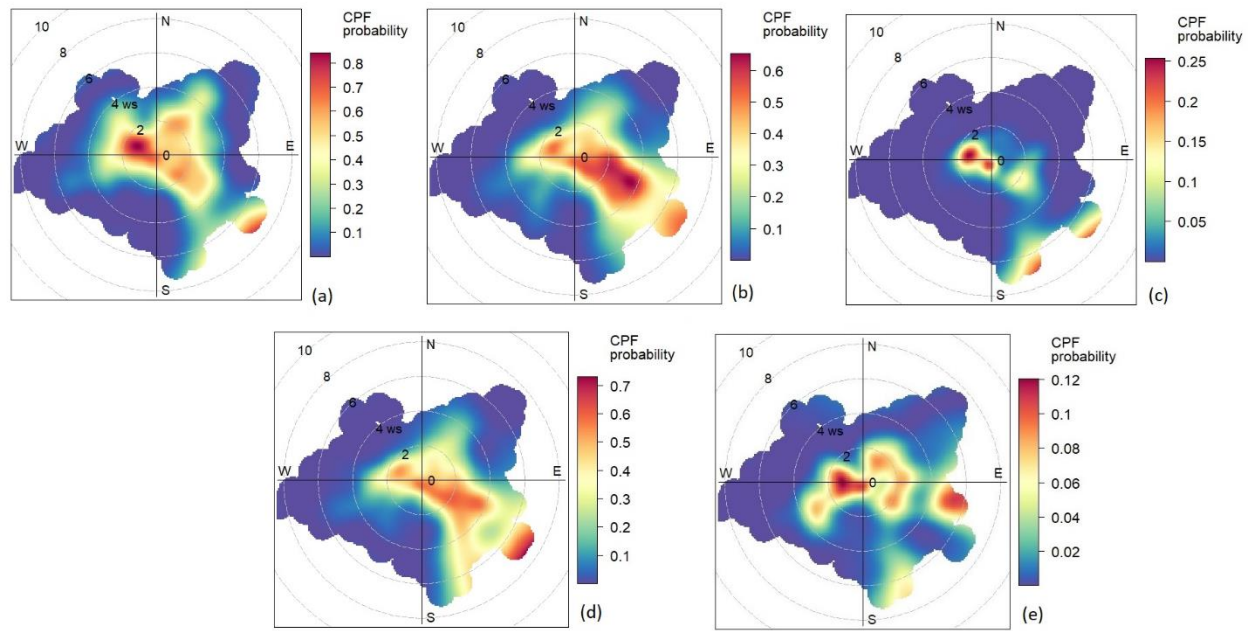
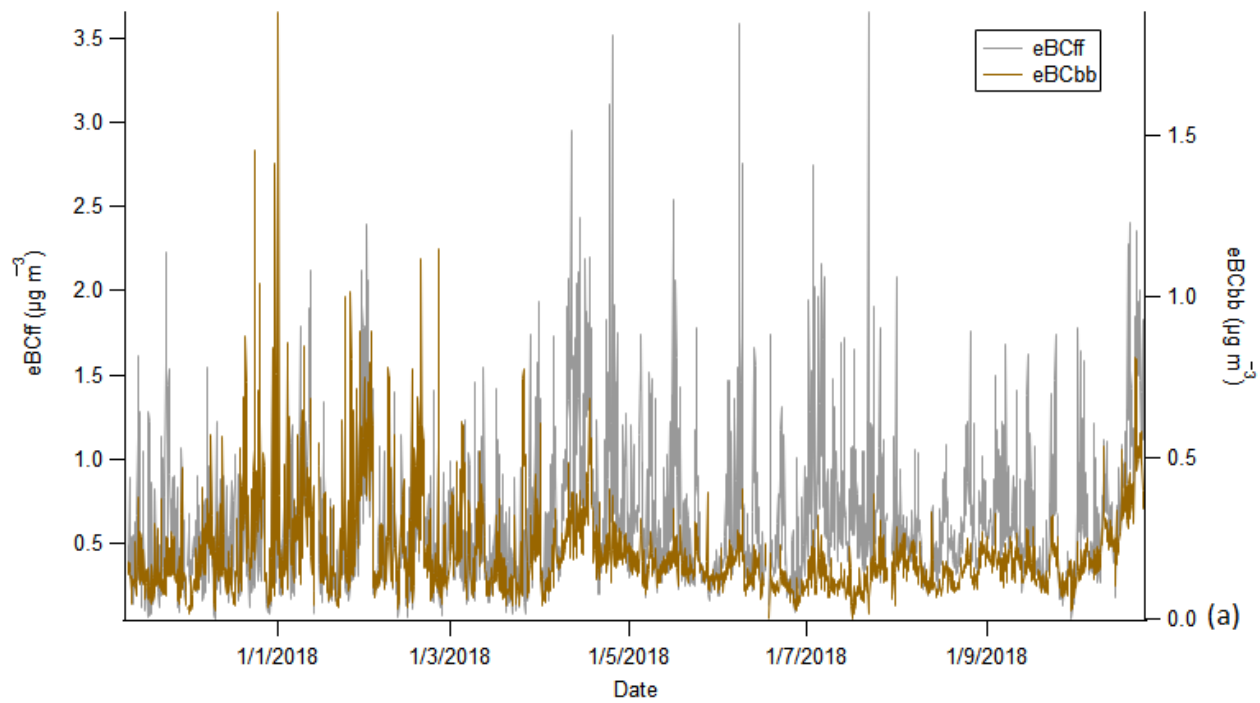
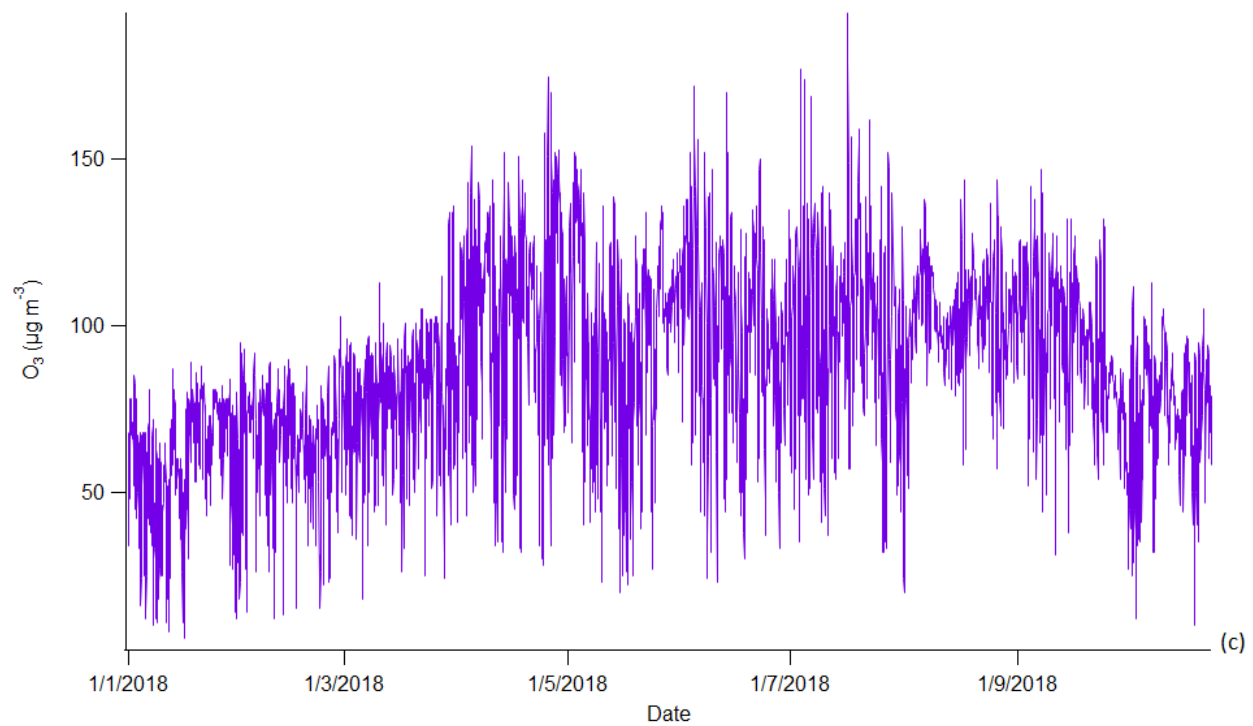
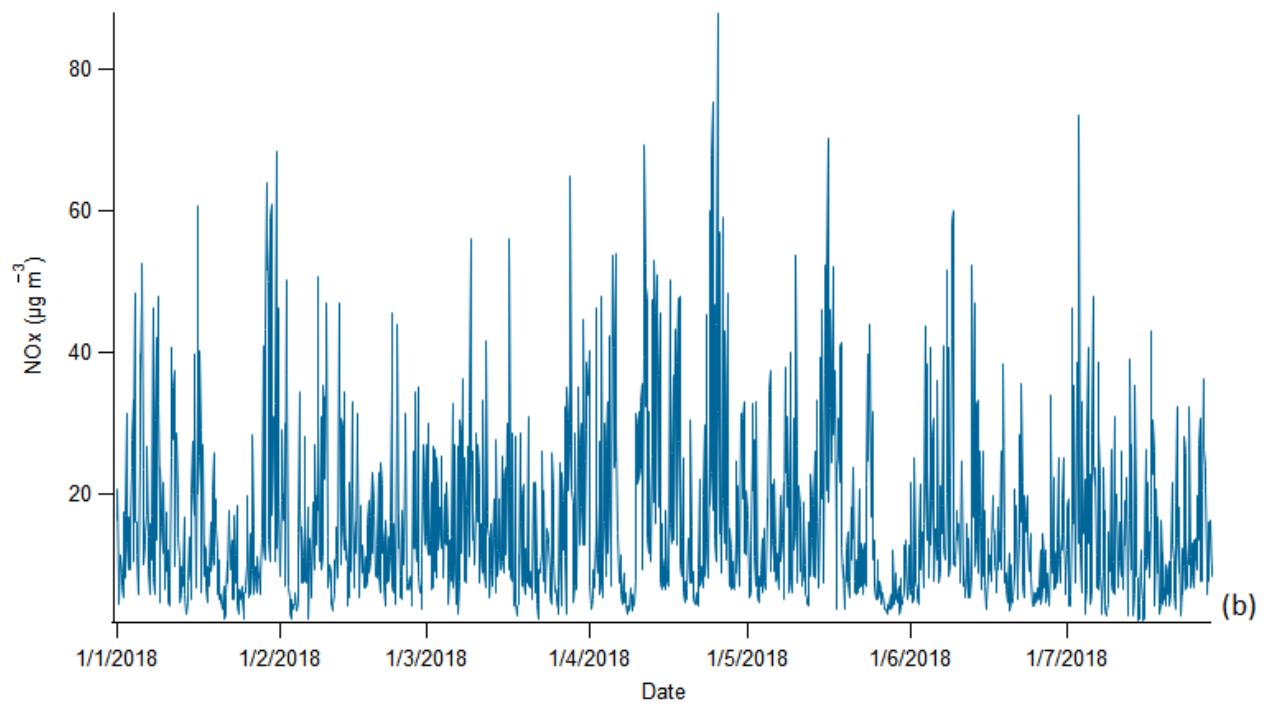
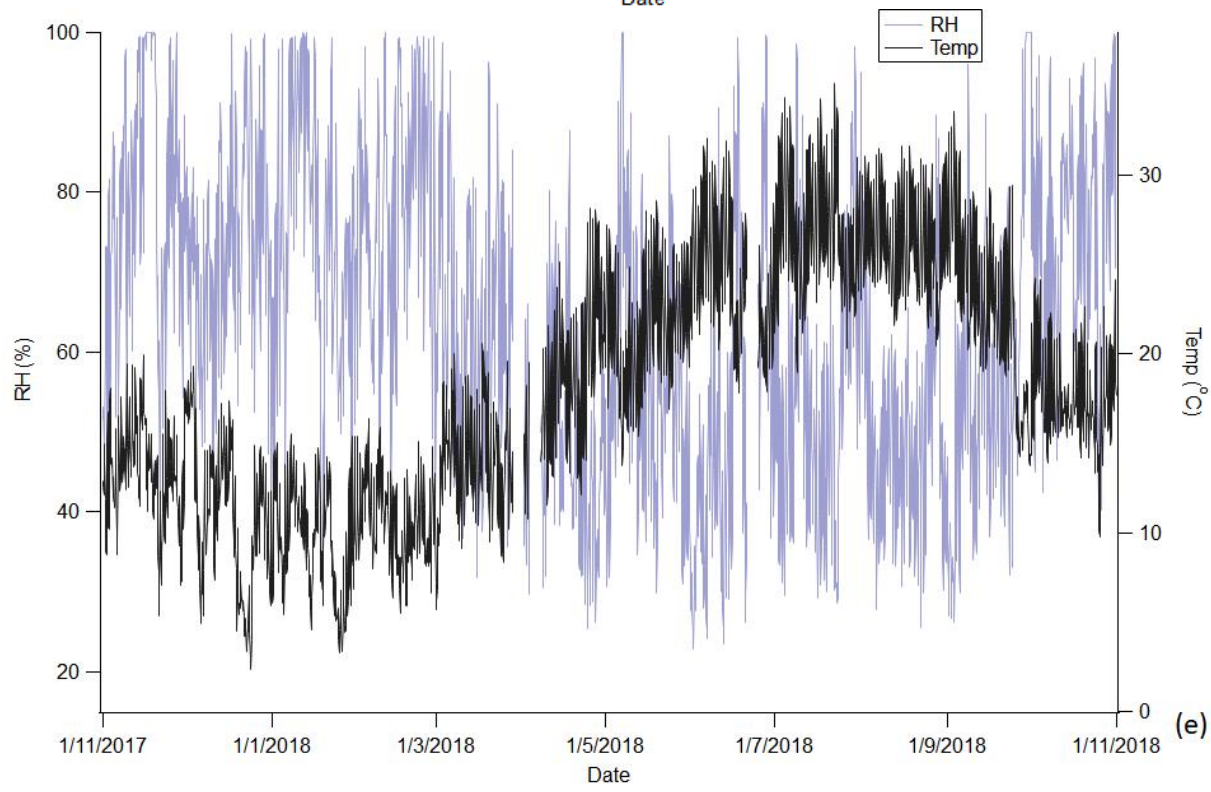
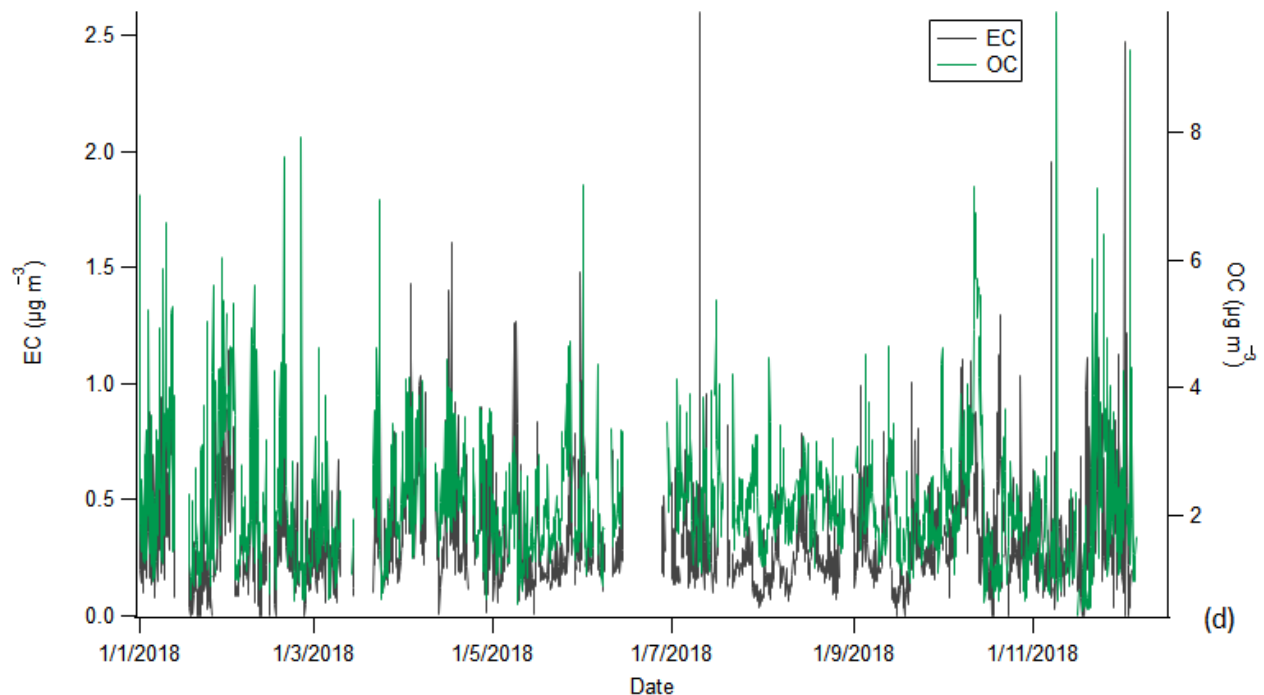


Figure S4. CPF polar plots for NRS: Org (a), SO₄ (b), NO₃ (c), NH₄ (d) and Cl (e).







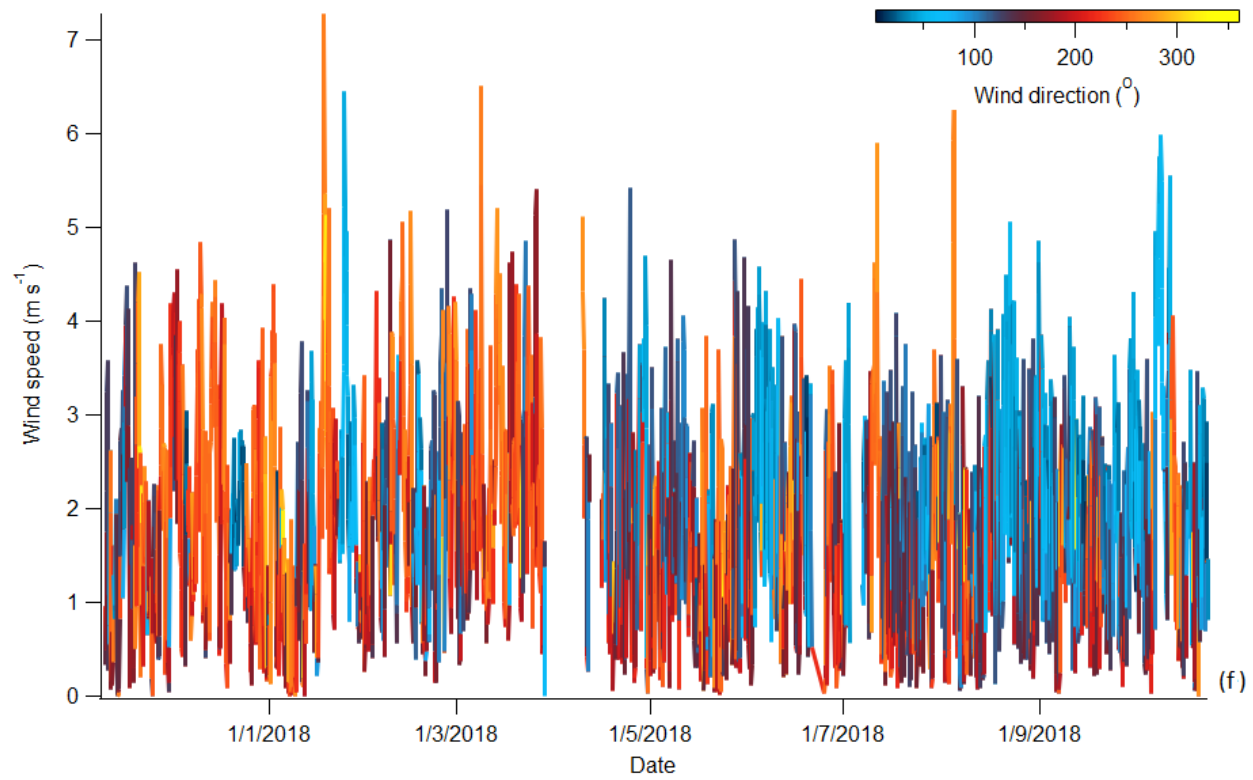


Figure S5. Supplementary data: equivalent black carbon apportioned to fossil fuel (eBC_{ff}) and wood burning (eBC_{wb}) (a), NOx (b), O₃ (c), EC/OC (d), relative humidity and air temperature (e) and wind speed and direction (f).

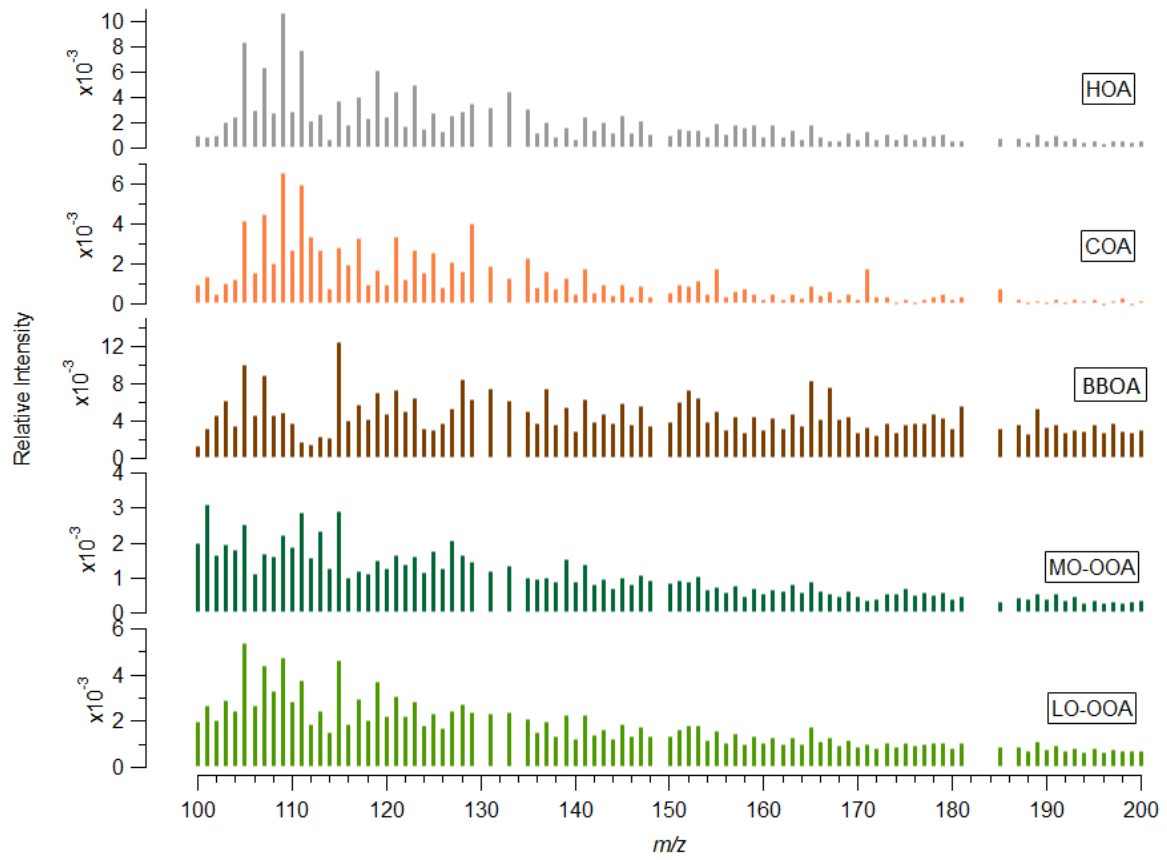
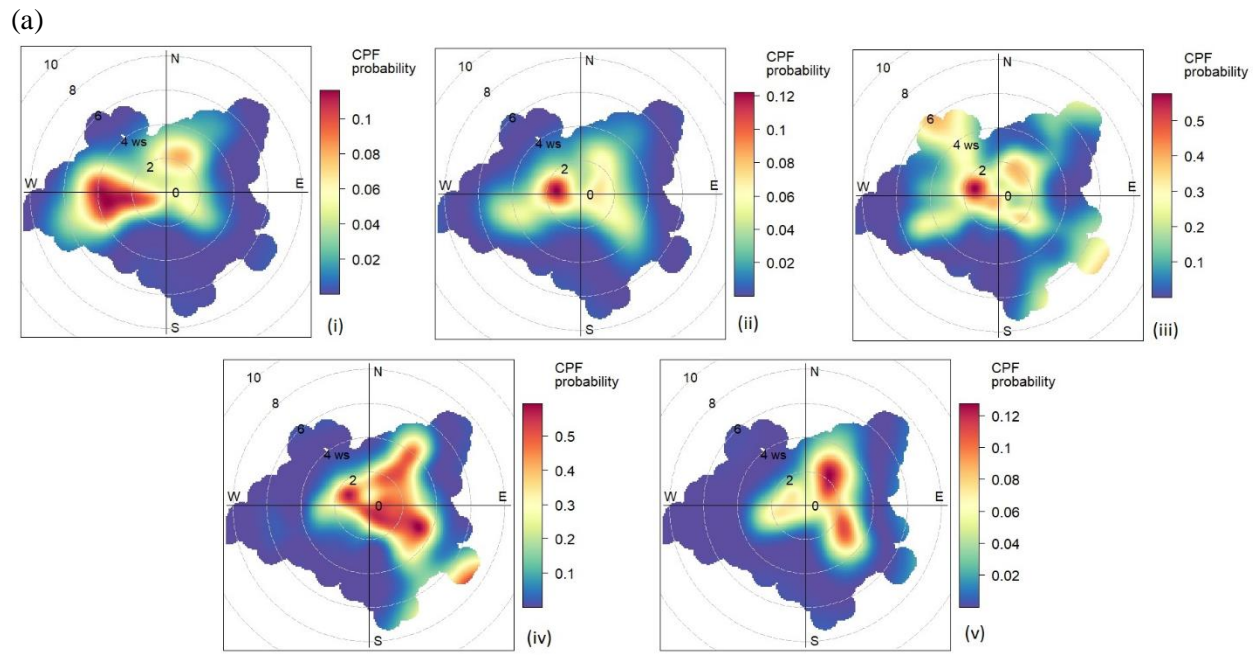


Figure S6. Mass spectrum of the five OA factors for mass to charge ratios 100 to 200.



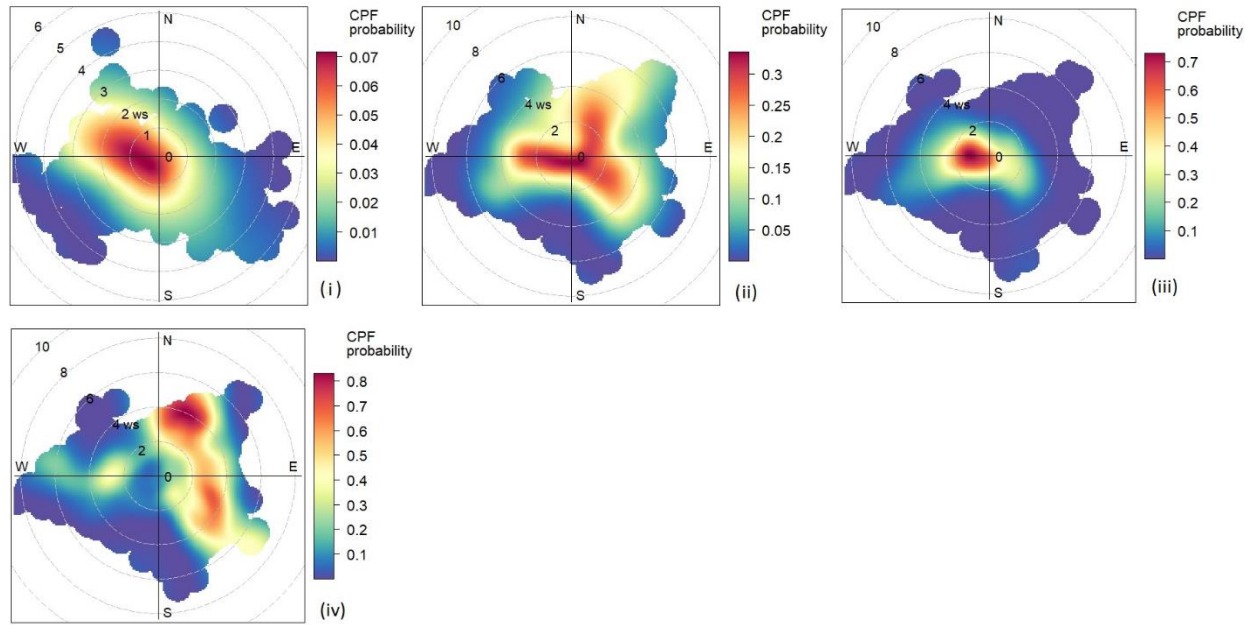


Figure S7. CPF polar plots for (a) organic aerosol factors (HOA (i), COA (ii), BBOA (iii), LO-OOA (iv) and MO-OOA (v)) and (b) external data (eBCff (i), eBCbb (ii), NOx (iii) and O₃ (iv)).

Table S3. Relative contribution and actual mass loading of each organic factor in each period studied.

	% / $\mu\text{g m}^{-3}$	Yearly	NDJF	MAM	JJA	SO
HOA	15 / 0.7	18 / 0.7	18 / 0.9		13 / 0.7	10 / 0.5
COA	18 / 0.8	19 / 0.8	19 / 1		16 / 0.8	14 / 0.7
BBOA	9 / 0.4	18 / 0.7	7 / 0.4		5 / 0.2	6 / 0.3
MO-OOA	34 / 1.6	31 / 1.3	33 / 1.6		35 / 1.8	39 / 1.8
LO-OOA	24 / 1.1	14 / 0.6	23 / 1.2		31 / 1.6	31 / 1.4

Table S4. R-Pearson correlations between organic aerosol factors and external tracers.

R-Pearson	Yearly	NDJF	MAM	JJA	SO
HOA/eBCff	0.69	0.68	0.78	0.70	0.67
HOA/NOx	0.69	0.56	0.73	0.75	N.A.
HOA/EC	0.58	0.53	0.66	0.55	0.53
BBOA/eBCwb	0.74	0.81	0.53	0.50	0.76
MO-OOA/SO₄²⁻	0.67	0.63	0.67	0.44	0.76
MO-OOA/NH₄⁺	0.7	0.74	0.68	0.46	0.77
MO-OOA/NO₃⁻	0.35	0.52	0.32	0.39	0.76
LO-OOA/SO₄²⁻	0.53	0.33	0.47	0.46	0.79
LO-OOA/NH₄⁺	0.52	0.43	0.54	0.5	0.8
LO-OOA/NO₃⁻	0.33	0.43	0.59	0.79	0.78

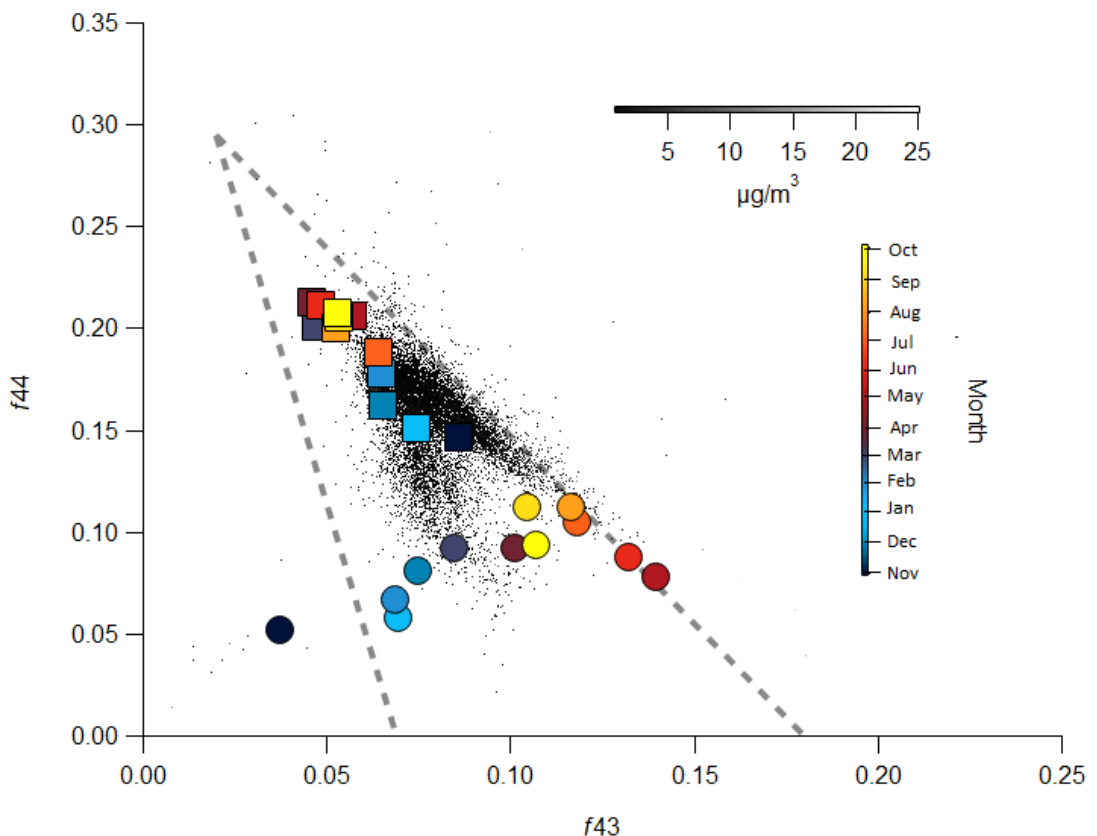


Figure S8. Subtracted f44-f43 plot for OA factors analyses (rectangles on the upper size: MO-OOA, cycles on the lower size: LO-OOA and points in the middle: OA data).

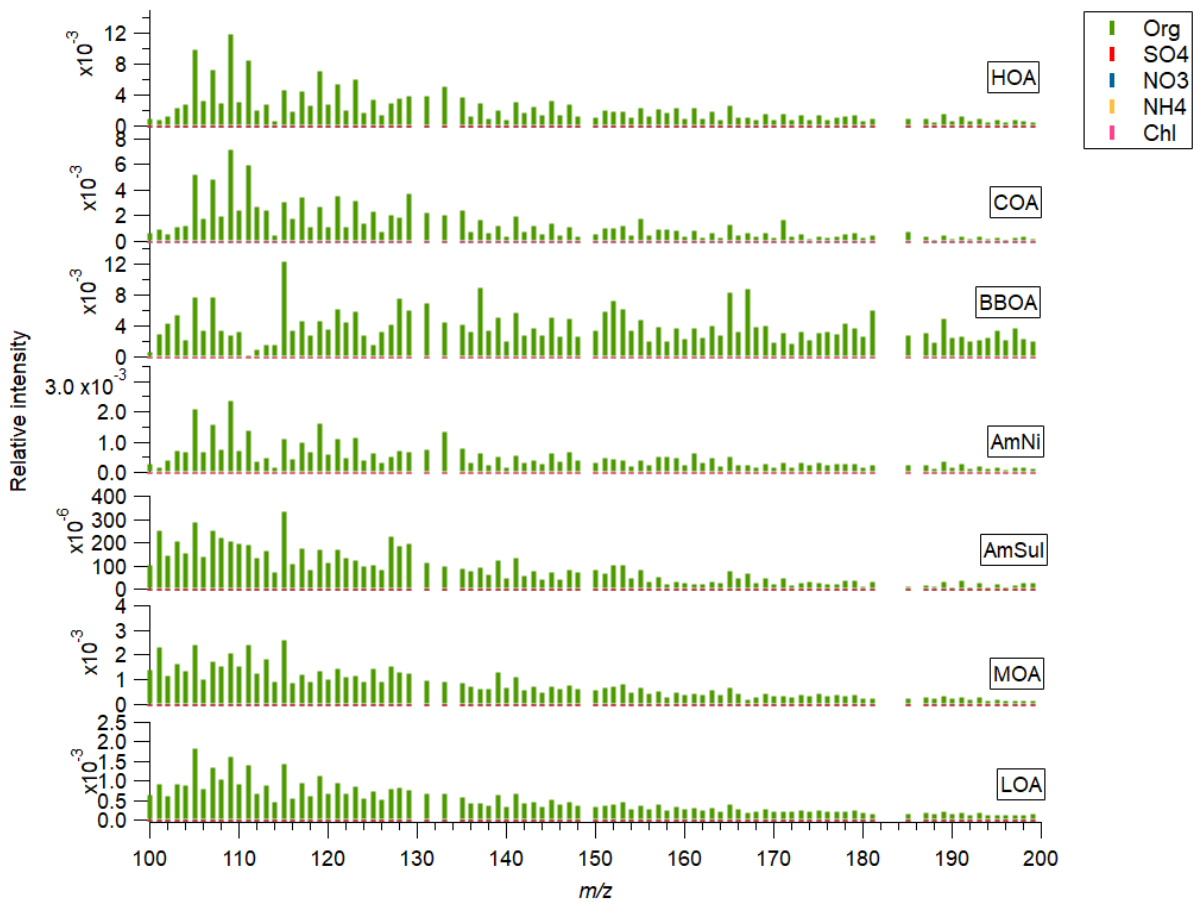


Figure S9. Mass spectrum of the seven NRS factors for mass to charge ratios 100 to 200.

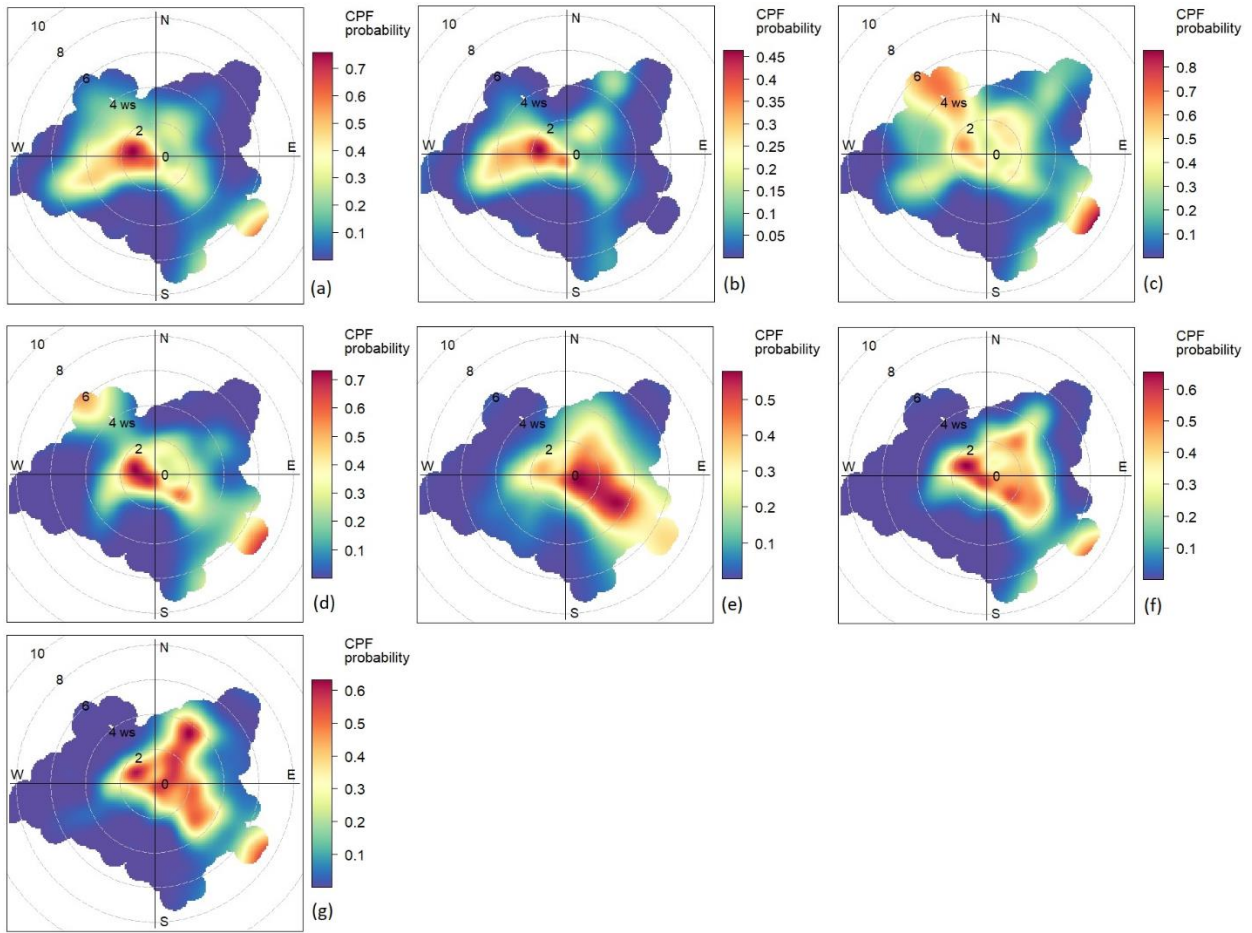


Figure S10. CPF polar plots for NRS factors from combined PMF analysis: HOA (a), COA (b), BBOA (c), AmNi (d), AmSul (e), LOA (f) and MOA (g).

Table S5. Relative contribution and actual mass loadings of each NRS factor in each period studied.

	% / $\mu\text{g m}^{-3}$	Yearly	NDJF	MAM	JJA	SO
HOA		7 / 0.6	9 / 0.6	8 / 0.7	5 / 0.5	4 / 0.4
COA		9 / 0.8	11 / 0.7	10 / 0.9	8 / 0.8	5 / 0.5
BBOA		3 / 0.3	9 / 0.6	3 / 0.2	2 / 0.2	2 / 0.2
AmNi		3 / 0.3	6 / 0.4	5 / 0.4	2 / 0.1	1 / 0.2
AmSul		28 / 2.4	21 / 1.3	27 / 2.5	27 / 2.6	35 / 3.6
MOA		24 / 2.1	25 / 1.6	24 / 2.1	27 / 2.7	20 / 2.1
LOA		26 / 2.2	19 / 1.2	23 / 2	29 / 2.9	33 / 3.4

Table S6. R-Pearson correlations between NRS aerosol factors and external tracers.

R-Pearson	Yearly	NDJF	MAM	JJA	SO
HOA/eBCff	0.7	0.67	0.84	0.74	0.66
HOA/NOx	0.75	0.59	0.82	0.77	-
HOA/EC	0.64	0.68	0.73	0.59	0.44
BBOA/eBCwb	0.75	0.84	0.51	0.46	0.68
MOA / OC	0.77	0.81	0.74	0.75	0.86
MOA / SO₄²⁻	0.47	0.31	0.53	0.33	0.5
MOA / MO-OOA	0.86	0.88	0.88	0.83	0.86
LOA/ SO₄²⁻	0.74	0.73	0.75	0.52	0.97
LOA/ NH₄⁺	0.74	0.74	0.76	0.49	0.96
LOA/ LO-OOA	0.68	0.41	0.73	0.4	0.83

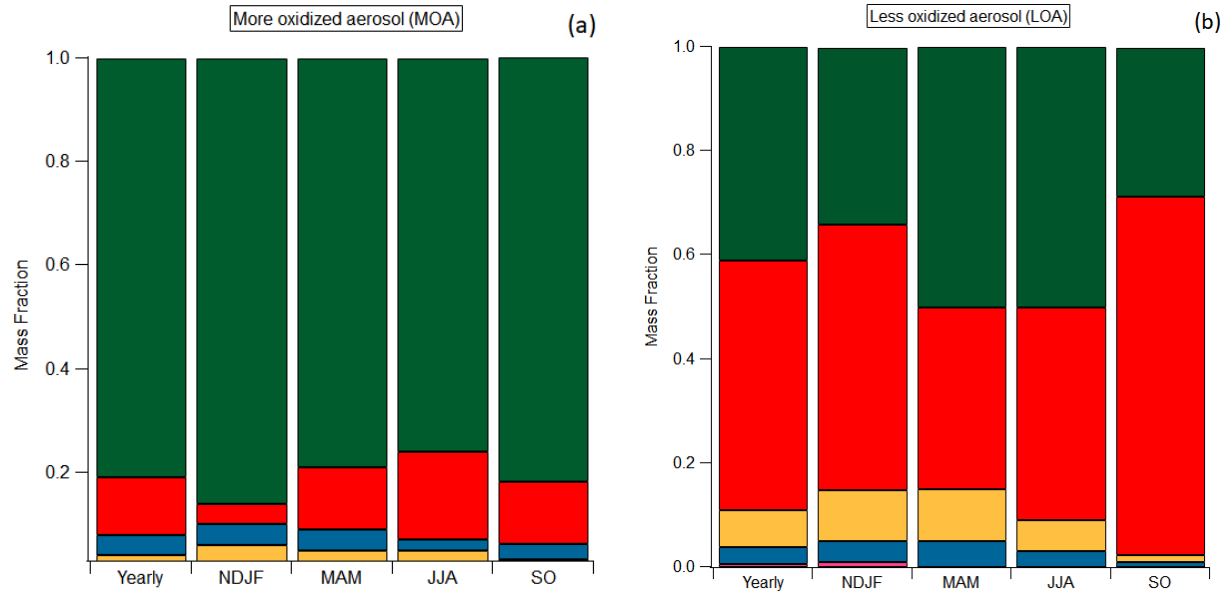


Figure S11. Mass fraction of each species in MOA (a) and LOA (b) in different seasons: Yearly, November–February (NDJF), March–May (MAM), June–August (JJA) and September–October (SO).

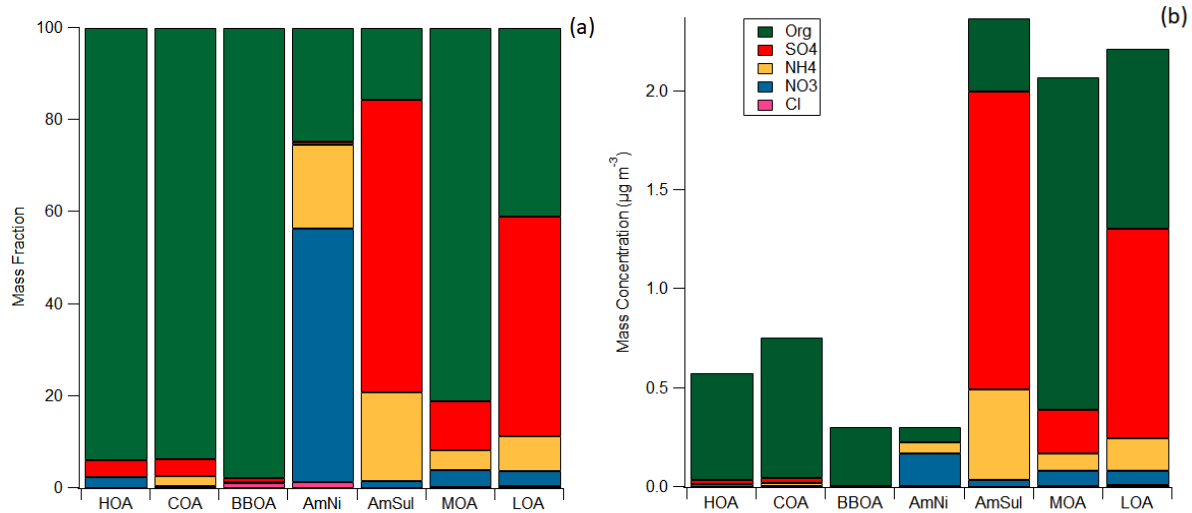


Figure S12. Mass fraction (a) and absolute concentration (b) of each species in each NRS factor.

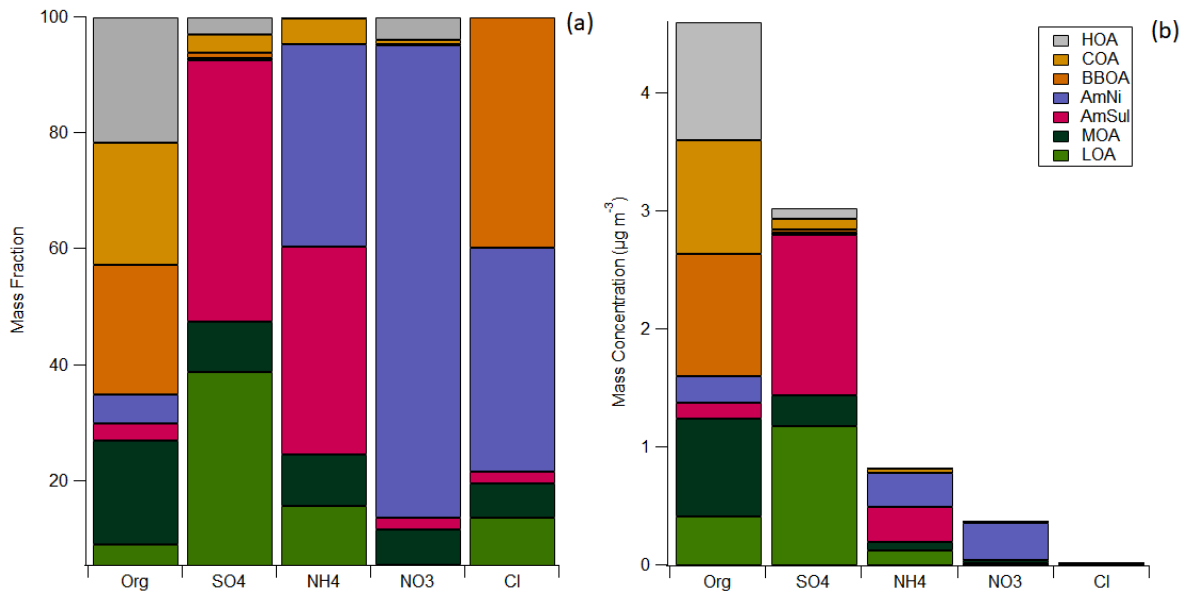


Figure S13. Mass fraction (a) and absolute concentration (b) of each NRS factor in each species.